



# Obtaining Material Properties from Indentation Loading-Unloading Curves using Simplified Equations

J.J. Kang, M. Boris, A.A. Becker and W. Sun  
Department of Mechanical, Materials and Manufacturing Engineering  
University of Nottingham, United Kingdom

## Abstract

In this study, a new approach is developed for extracting elastic-plastic material properties from the indentation loading-unloading curves by using different indenter geometries (conical and Vickers indenters) and different indenter angles ( $60^\circ$  and  $70.3^\circ$ ). Mathematical functions that fit the loading-unloading curves are introduced and a MATLAB nonlinear least square routine with practical equality and inequality constraints is used to extract the elastic-plastic material properties based on the best fit between the target load-displacement curve, obtained using finite element (FE) analysis, and the predicted optimized curves. In order to obtain the accurate optimized results, intermediate ‘focus tests’ are introduced and the optimized results are shown to be in good agreement with the target values.

**Keywords:** indentation, optimization, elastic-plastic properties.

## 1 Introduction

Indentation testing is a successful technique for measuring hardness and elastic properties from loading-unloading force-displacement curves. The instrumentation of indentation tests and the analysis of the resulting data have been extensively developed in the last two decades. In previous work, the authors have focused on the evaluation of elastic-plastic material properties based on dimensional analysis [1] and FE simulations [2]; both methods are based on non-linear optimization techniques. However, extensive computational times are required for the FE analyses due to the fact that the optimization procedure is based on iterative FE computations [2]. Since the characteristic indentation loading-unloading response can be described by dimensional analysis [1], more simplified approaches which do not require iterative FE analyses can be devised to obtain the elastic-plastic mechanical properties from experimental loading-unloading curves, based on the optimization technique.

The objective of this study is to present an improved approach for extracting the elastic-plastic material properties from the indentation loading-unloading curves. Based on the Olive-Pharr method [3], the complicated mathematical equations based on dimensional analysis can be simplified. The mathematical functions involve material parameters (Young's modulus, yield stress and post-yield work hardening exponent). The simulated target load-displacement curves using different indenter geometries (conical and Vickers indenters) and different indenter angles ( $60^\circ$  and  $70.3^\circ$ ) can be obtained from FE analysis. For predicting the sets of material properties from the loading-unloading curves, a MATLAB nonlinear least square routine with practical equality and inequality constraints [4] is used to produce the best fit between the simulated target load-displacement curve and the predicted optimized curves.

## 2 Framework of Analysis

A typical loading-unloading curve of an elastic-plastic material subjected to an instrumented sharp indentation is presented in Figure 1.

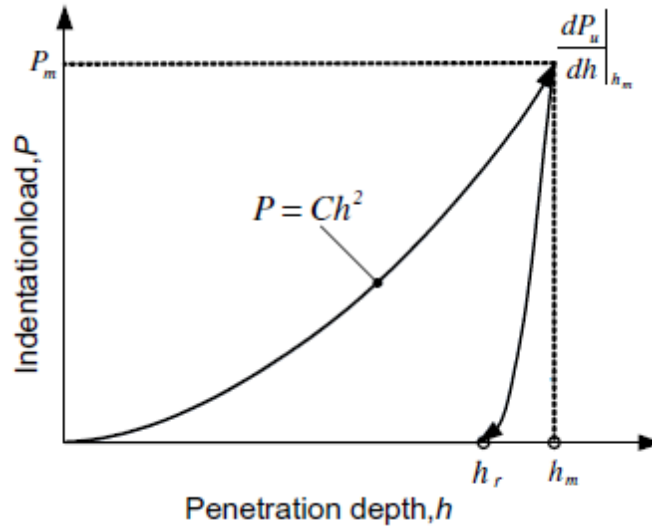


Figure 1 Typical load-displacement curve of an elastic-plastic material subjected to a sharp indentation. [3]

The loading portion of the curve can be described by Kick's Law [3], i.e.

$$P = Ch^2 \quad (1)$$

where  $C$  is the loading curvature which is related to the geometry of the indenter tip and the material properties of the test material. The maximum applied indenter displacement,  $h_m$ , occurs at the maximum load,  $P_m$ ,  $h_r$  is the final residual depth after the indenter is completely removed and the initial unloading slope can be

expressed by  $S = \left. \frac{dP_u}{dh} \right|_{h_m}$ , where  $P_u$  is the unloading load. The hardness of a material can be determined from the maximum load and the elastic modulus can be determined from the initial part of the unloading curve, referred to as the contact stiffness. From the unloading data, the contact area and the plastic depth of penetration can be obtained. Therefore, the unloading stiffness is the most significant part of an indentation load-displacement loop since it is significantly dependent on the elastic properties of the materials. Oliver and Pharr [3] observed that the unloading curve is usually well represented by a power law fit as follows:

$$P = A(h - h_r)^m \quad (2)$$

$$S = \left( \frac{dP}{dh} \right)_{h=h_{\max}} = Am(h_{\max} - h_r)^{m-1} \quad (3)$$

where  $m$  is the power law index, and  $A$  is a constant. The five independent governing parameters  $C$ ,  $S$ ,  $A$ ,  $m$ ,  $h_r / h_{\max}$  and  $h_r$  can be directly obtained from a single loading-unloading curve. This suggests that those parameters can be used to obtain unknown material properties from loading-unloading curves based on an optimization approach. According to the Buckingham  $\pi$ -theorem for dimensional analysis [5, 6], the dimensional scaling relationship for the indentation loading curvature can be expressed as

$$P_{\text{Loading}} = \sigma_r f_1 \left( \frac{E^*}{\sigma_r}, n \right) h^2, \quad (4)$$

and thus

$$C = \frac{P}{h^2} = \sigma_r f_1 \left( \frac{E^*}{\sigma_r}, n \right), \quad (5)$$

where  $f_1$  is a dimensionless function, where the normalization is taken with respect to  $\frac{E^*}{\sigma_r}$ . The reduced Young's modulus is given by:

$$\frac{1}{E^*} = \frac{1 - \nu_s^2}{E_s} + \frac{1 - \nu_i^2}{E_i} \quad (6)$$

where  $E_s, E_i, \nu_s$  and  $\nu_i$  are the elastic modulus and Poisson's ratio of the specimen and indenter, respectively. The Poisson's ratio of the specimen is fixed as 0.30. For a "rigid" indenter, the second term in Eq. (6) is negligible. Therefore, Eq. (6) can be rewritten as follows:

$$\frac{1}{E^*} = \frac{1 - \nu_s^2}{E_s} \quad (7)$$

For the unloading curve, the relationship between the normalised  $\frac{F_{max}}{(h_m - h_r)^m}$  and  $A$ , and the relationship between the normalised  $\frac{mF_{max}}{(h_m - h_r)}$  and the initial slope of unloading curve,  $S$  can be obtained from a parametric study, as discussed by Kang et al [1]. From those relationships, constant  $A$  and  $m$  in Eq. (2) can be expressed as following:

$$A = \frac{F_{max}}{(h_{max} - h_r)^m} \quad (8)$$

$$S = \frac{dF}{dh} = \frac{mF_{max}}{(h_{max} - h_r)} \quad (9)$$

which can be rewritten as

$$m = \frac{S(h_{max} - h_r)}{F_{max}} \quad (10)$$

From Dao's study [5], the dimensional scaling relationship for the final residual depth can be expressed when the unloading force is zero

$$\frac{h_r}{h_m} = f_2 \left( \frac{\sigma_r}{E^*}, n \right) \quad (11)$$

Since the relationships of the loading-unloading response of the indenter are known, the equation covering the loading and unloading portion of the curves can be assumed as follows:

$$C = \sigma_r k_1 \left( \log \left( \frac{E^*}{\sigma_r} \right) \right) \quad (12)$$

and when substituted into eq.(1), can be expressed as follows:

$$P_{Loading} = \sigma_r k_1 \left( \log \left( \frac{E^*}{\sigma_r} \right) \right) h^2 \quad (13)$$

$$\text{where, } \sigma_r = \sigma_y \left( 1 + \frac{E}{\sigma_y} 0.0115 \right)^n$$

where  $h$  is the displacement of indenter,  $\sigma_y$  is initial yield stress,  $E$  is Young's modulus and  $n$  is work-hardening exponent. Moreover, the final residual depth of the indenter,  $h_r$ , can be assumed as follows:

$$h_r = h_m n k_2 \left( \log \left( \frac{E^*}{\sigma_r} \right) \right) \quad (14)$$

where  $h_m$  is the maximum displacement of the indenter.

The elastic-plastic behaviour for many pure and alloyed engineering metals can be expressed by a power law relationship, which is presented schematically in Figure 2. The stress-strain ( $\sigma_r - \epsilon$ ) relationship [7] is assumed to be

$$\sigma_r = \begin{cases} E\epsilon & \text{for } \epsilon \leq \frac{\sigma_y}{E} \\ R\epsilon^n & \text{for } \epsilon > \frac{\sigma_y}{E} \end{cases} \quad (15)$$

where  $R$  is a strength coefficient and  $\sigma_y$  is the stress at zero offset strain. The decomposition of the total strain is given by

$$\epsilon_{\text{total}} = \epsilon_{\text{el}} + \epsilon_{\text{pl}} \quad (16)$$

where  $\epsilon_{\text{el}}$  is the elastic strain component and  $\epsilon_{\text{pl}}$  is the plastic strain component.

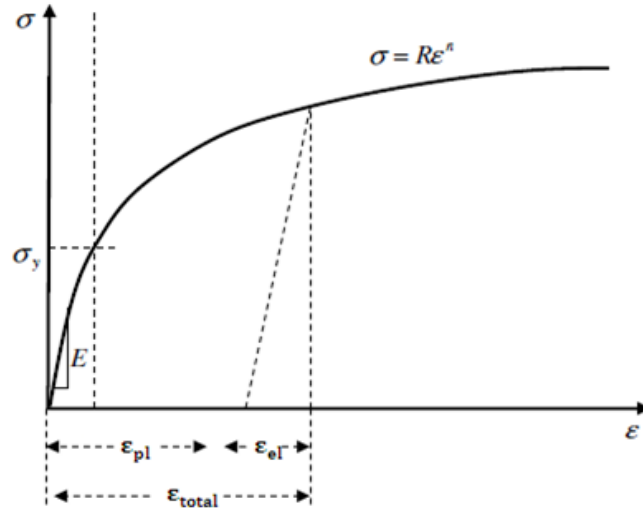


Figure 2 Power law elasto-plastic stress-strain behaviour

The stress equation can be written as

$$\sigma_r = R \left( \frac{\sigma_y}{E} + \epsilon_{\text{pl}} \right)^n \quad (17)$$

where the coefficient  $R$  is given by  $R = E^n \sigma_y^{1-n}$  and  $\sigma_r$  is called the representative stress. Therefore, three material parameters ( $E, \sigma_y, n$ ) are needed to describe the power law elastic-plastic behaviour of the material. Ogasawara et al. [8] have found that a representative strain  $\varepsilon_{pl} = 0.0115$  can be identified for the conical indenter ( $\alpha = 70.3^\circ$ ) within a specified range of material parameters. The representative strain  $\varepsilon_r = 0.0115$  can be applied to essentially all power-law engineering materials and the dimensionless relationship between  $C / \sigma_y \langle \varepsilon_r \rangle$  and the  $E^* / \sigma_y \langle \varepsilon_r \rangle$  are practically independent of  $n$ . Therefore, the representative strain  $\varepsilon_r = 0.0115$  can be used in this study.

### 3 Finite Element Modelling

The ABAQUS [9] FE code is used in this study to obtain a simulated indentation loading-unloading curve. The conical indenter is modelled as an axisymmetric geometry using three-node axisymmetric triangular linear continuum elements (CAX3 in ABAQUS) and four-node axisymmetric quadrilateral linear continuum elements with reduced integration (CAX4R in ABAQUS). The Vickers indenter is modelled as a 3D geometry with a high element density of four-node linear tetrahedron continuum elements (C3D4 in ABAQUS). For the rigid indenters, a four-node 3-D bilinear rigid quadrilateral continuum element (R3D4 in ABAQUS) is utilized. Contact is prescribed between the rigid indenters and the elastic-plastic specimen. The assumption of a perfectly sharp indenter is employed. A “master-slave” contact scheme in the FE procedure is applied on the rigid indenter and the specimen surface. The friction coefficient at the contact surface between the indenter and the top surface of the substrate is assumed to be zero, since friction has a negligible effect on the indentation process [10]. The region of interest is in the vicinity of the indenter tip where a high element density has been used due to the very high stress gradients immediately beneath the indenter tip. Typical FE meshes, arrived at by a mesh convergence study, are shown in Figure 3.

The indentation simulations are carried out in two distinct steps, loading and unloading. In the first step, a total indenter displacement of 0.002 mm is imposed. During loading, a rigid indenter moves downwards along the loading axis and penetrates the foundation up to a maximum specified depth. In the second step, the indenter is unloaded and taken back to its initial position. Table 1 presents the material properties used to obtain the simulated indentation loading-unloading curve.

Obtaining a unique set of material properties of a power-law material from a single indentation test has proved to be difficult. Consequently, some researchers [11, 12, 13 and 14] have used load-displacement curves obtained from more than one indenter geometry (dual indenters) in order to obtain a unique set of material constants. It has been shown that decreasing the indenter angle, i.e. using a sharper tip geometry, improves the accuracy of estimation of the mechanical properties [11].

The simulated target load-displacement curve using different indenter geometries (conical and Vickers indenters) and different angles ( $60^\circ$  and  $70.3^\circ$ ) have been obtained from FE analysis, as shown in Figure 4.

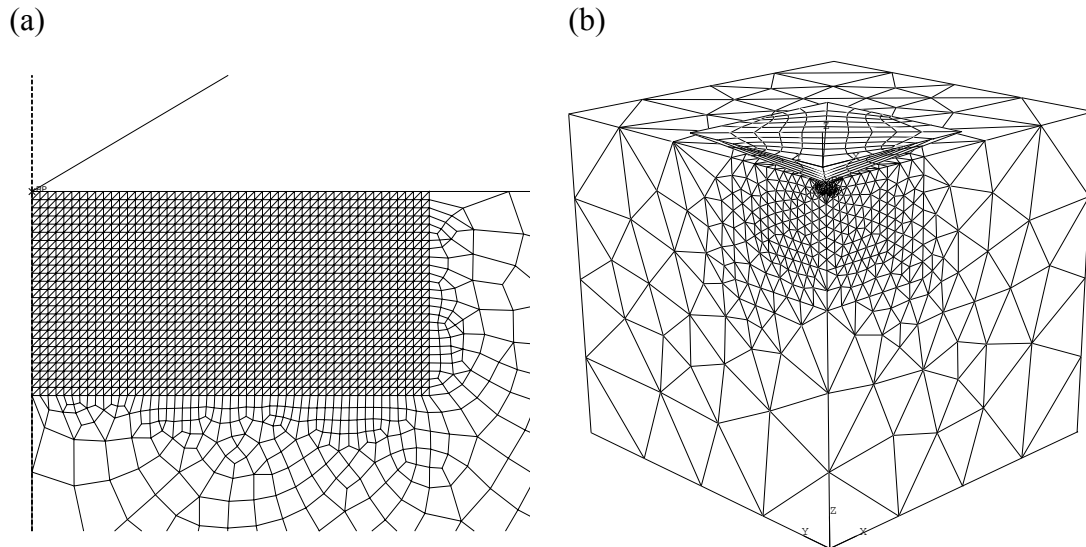


Figure 3 Typical FE meshes used in the indentation analysis (a) axisymmetric conical indenter (b) 3D Vickers indenter

Case	Young's modulus, E	Yield stress, $\sigma_y$	Work hardening exponent, n
1	50 GPa	300 MPa	0.1
2	100 GPa	900 MPa	0.5
3	210 GPa	900 MPa	0.3

Table 1 Material properties used to obtain the simulated indentation curves

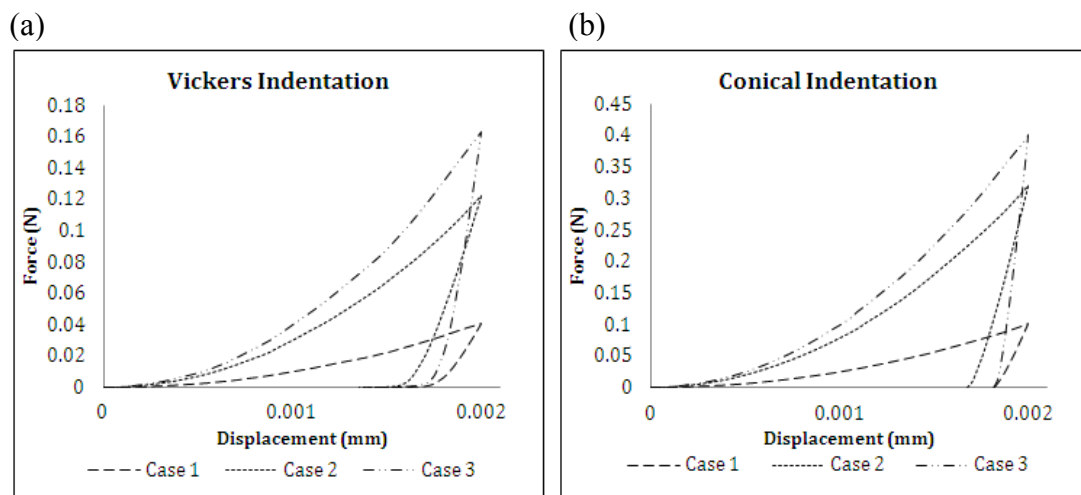


Figure 4 Load displacement indentation curves of the three material cases for (a) Vickers and (b) conical indenters with a face angle of  $70.3^\circ$

## 4 An optimization procedure for determining material properties

### 4.1 Optimization model

For predicting the sets of material properties from the loading-unloading curve, the MATLAB Fmincon function with interior-point algorithm and nonlinear least square routine with practical equality and inequality constraints is used to produce the best fit between the simulated target load-displacement curve and the predicted optimized curves. In order to reduce the set of optimization parameters, Eq. (14) is substituted into Eq. (12) resulting in:

$$k_1 = \frac{Ch_m n k_2}{h_r \sigma_r} \quad (18)$$

Furthermore, the relationship of the ‘k’ terms between axisymmetric and 3D Vickers indenters is assumed as follows:

$$\frac{k_1 k_{2 \text{ for 1st indenter}}}{k_{11} k_{22 \text{ for 2nd indenter}}} = \frac{C_1 h_{r1 \text{ for 1st indenter}}}{C_{11} h_{r11 \text{ for 2nd indenter}}} \quad (19)$$

$$k_{11} = k_1 C_{11} / C_1 \quad (20)$$

$$k_{22} = k_2 h_{r11} / h_{r1} \quad (21)$$

where,  $C_1$  and  $C_{11}$  are loading curvatures and  $h_{r1}$  and  $h_{r11}$  are the final residual depths of the indenters for the 1<sup>st</sup> indenter and the 2<sup>nd</sup> indenter, respectively. The angles of 1<sup>st</sup> and 2<sup>nd</sup> indenters can be either 60° or 70.3° for the conical and Vickers indenters.

In this study, two different types of indenters are required in order to obtain the mechanical properties from the loading-unloading curves, but based on equations (19)-(21), only four different optimization variable sets ( $E, \sigma_y, n, k_2$ ) are required.

The optimization model [4] is:

$$F(x) = \frac{1}{2} \sum_{i=1}^N [P(x)_i^{\text{pre}} - P_i^{\text{exp}}]^2 \rightarrow \min \quad (22)$$

$$x \in R^n \quad (23)$$

$$LB \leq x \leq UB \quad (24)$$

where  $F(x)$  is the objective function,  $x$  is the optimization variable set (a vector in the  $n$ -dimensional space,  $R^n$ ), which for this specific case contains the full set of the material constants in the model, i.e.



$$x = [K_2, E, \sigma_y, n]^T \quad (25)$$

and  $LB$  and  $UB$  are the lower and upper boundaries of  $x$  allowed during the optimization. For example, the work-hardening exponent values for most engineering materials are between 0.1 and 0.5. A limited range of material properties are chosen in this study and lower and upper limits have been imposed on the values of Young's modulus between 10 GPa to 210 GPa and yield stress values between 10 MPa and 2500 MPa in order to cover all practical engineering materials during the optimization procedures [15].  $P(x)_i^{\text{pre}}$  and  $P_i^{\text{exp}}$  are the predicted indentation force and the experimental force from the target data, respectively, at a specific position  $i$ , within the loops.  $N$  is the total number of points used in the measured loading-unloading loop. Arbitrary values of  $(K_2, E, \sigma_y, n)$  have been chosen as initial values and the proposed optimization algorithm has been used to find the optimized values of  $K_2, E, \sigma_y$  and  $n$  from which the best fits between the experimental and predicted loading-unloading curve can be achieved. Furthermore, some practical physical equality constraints have been imposed during the analysis, which is given by:

$$\left\{ \begin{array}{l} \frac{k_1 k_2 \text{ for 1st indenter}}{k_{11} k_{22} \text{ for 2nd indenter}} - \frac{C_1 h_{r1} \text{ for 1st indenter}}{C_{11} h_{r11} \text{ for 2nd indenter}} = 0 \\ S - Am(h_{\max} - h_r)^{m-1} \text{ for 1st \& 2nd indenter} = 0 \\ h_r - h_m n k_2 \left( \log \left( \frac{E^*}{\sigma_r} \right) \right) \text{ for 1st \& 2nd indenter} = 0 \end{array} \right. \quad (26)$$

where  $S$  and  $h_r$  can be obtained from analytical loading-unloading curves, based on the Oliver-Pharr method [3]. These assumptions are limited due to the fact that a parametric study of  $k_1$  and  $k_2$  values for a wide range of material properties and the bounds for those factors have not been performed. A relationship between these values can be devised as follows:

$$\frac{C_{\min}}{\sigma_r \log \left( \frac{E^*}{\sigma_r} \right)} \geq k_1 \geq \frac{C_{\max}}{\sigma_r \log \left( \frac{E^*}{\sigma_r} \right)} \quad (27)$$

$$\frac{h_r}{h_{\max} n \log \left( \frac{E^*}{\sigma_r} \right)} \geq k_2 \geq \frac{h_r}{h_{\max} n \log \left( \frac{E^*}{\sigma_r} \right)} \quad (28)$$

where  $C_{\min}$  and  $C_{\max}$  are the minimum and maximum values of the loading curvatures. The relationships of  $k_1 / k_2$  can be obtained by rearranging Eq. (27) and Eq. (28)

$$\frac{C_{min} h_{max} n}{h_r \sigma_r} \geq \frac{k_1}{k_2} \geq \frac{C_{max} h_{max} n}{h_r \sigma_r} \quad (29)$$

The above relationships can be calculated during the iterations, but the issue of uniqueness can arise due to the fact that the loading-unloading curves from different sets of material properties can be almost indistinguishable. Therefore, further investigation of the relationship between  $k_1$  and  $k_2$  factors and the geometry of indenter for a given material are required.

## 4.2 Optimization procedure

Previous studies have shown that, in many inverse approaches [5, 11-14], the elastic-plastic mechanical properties of a power-law material cannot be uniquely determined from a single indentation loading-unloading curve. Therefore, dual indenters have been used in this study. Since  $k_1$  and  $k_2$  factors are introduced in this study, the issues of uniqueness can arise despite using dual indenters. Therefore, a guideline for the optimization process in this study can be introduced to overcome this issue. The four different loading-unloading curves obtained from conical and Vickers indenters with  $60^\circ$  and  $70.3^\circ$  angles can be obtained from FE analysis. The five independent governing parameters ( $C$ ,  $S$ ,  $A$ ,  $m$ ,  $h_r / h_{max}$  and  $h_r$ ) can be directly obtained from the four different loading-unloading curves, which helps to address the issues of uniqueness.

In order to obtain the best optimized results, three types of ‘focus tests’ have been introduced. Vickers indenters with different face angles ( $60^\circ$  and  $70.3^\circ$ ) are used in the first focus tests. It is found that using the Vickers indenters gives better optimized results due to fact that the residual depths after unloading for different face angles ( $60^\circ$  and  $70.3^\circ$ ) are larger than those of the conical indenters. The second focus tests combine the Vickers indenter with  $60^\circ$  angle and the conical indenter with  $70.3^\circ$  angle. The third focus tests combine the Vickers indenter with  $70.3^\circ$  angle and the conical indenter with  $60^\circ$  angle. From the third focus tests, the best accuracy of the optimized values compared with the target values can be obtained. The new bounds of the mechanical parameters ( $K_2, E, \sigma_y, n$ ) and initial guess values can be changed, depending on the results from the focus tests.

The general optimization algorithm used in this study is illustrated in Figure 5. The initial guess parameters ( $K_2, E, \sigma_y, n$ ) should be chosen within the range of bounds mentioned in Section 4.1. As can be seen from Figure 5, the optimization loop is introduced in order to reduce the range of bounds during each loop. This means that the following loop will be always within updated range of bounds. It can also be used to check that the optimized results are unique within this updated range of bounds.

Figure 6 shows how the MATLAB optimization process is used with several simulations for one specimen. Firstly, the bounds and initial guess of the focus tests should be the same during all focus tests loops. Once all these trials have been

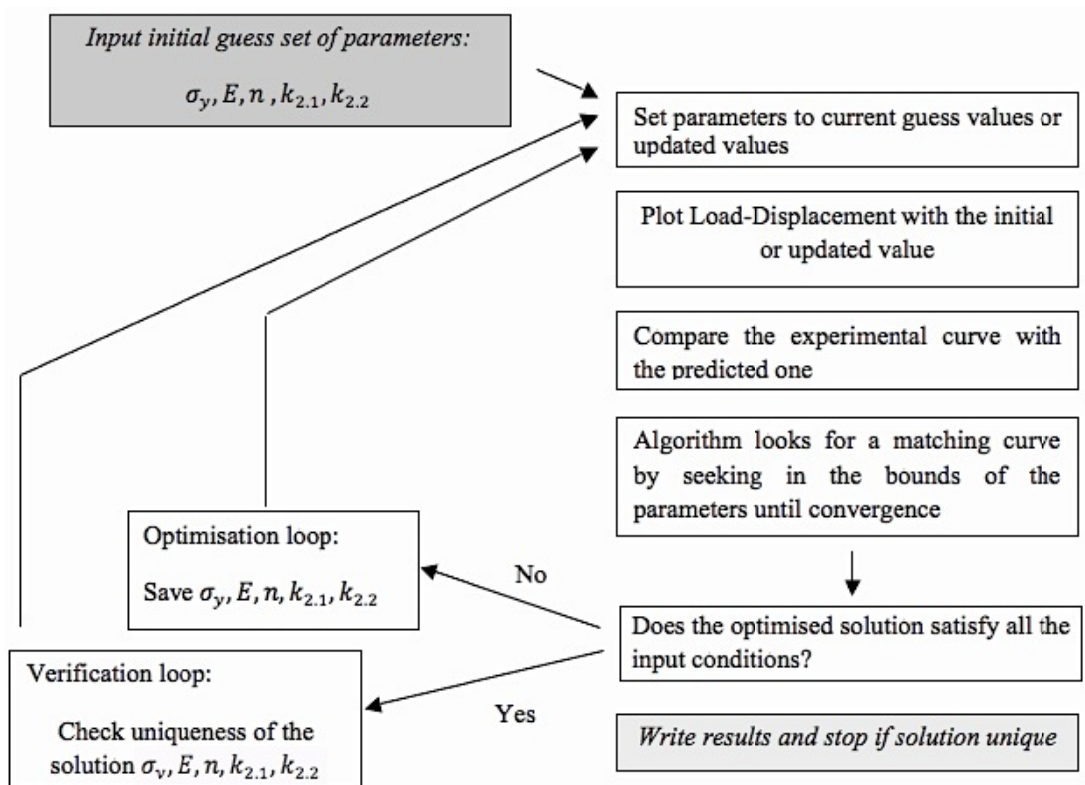


Figure 5 Flow chart of the optimization algorithm to determine the mechanical properties from the loading-unloading curve

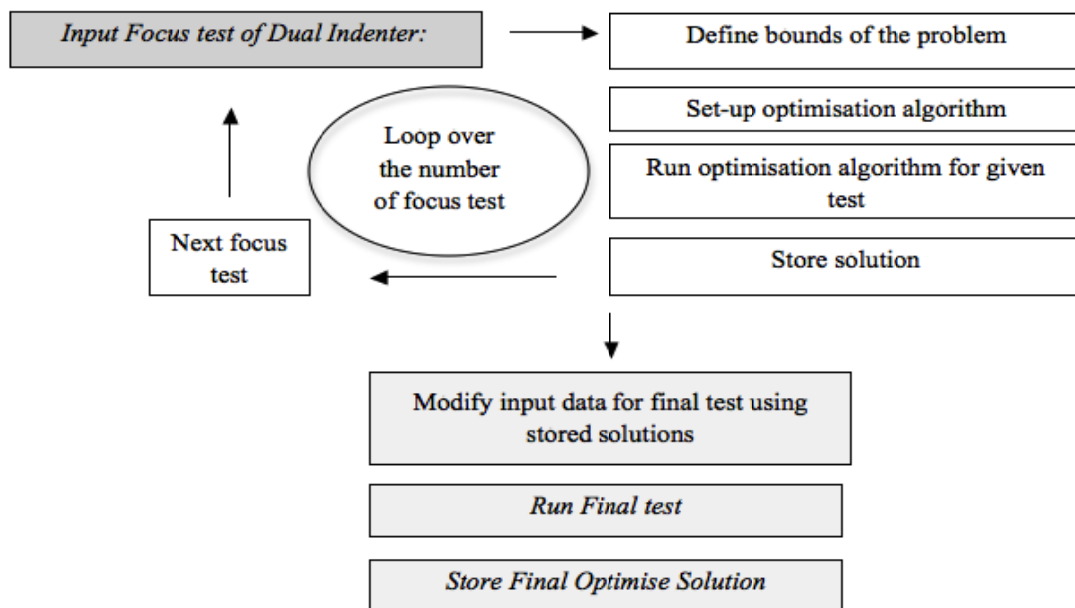


Figure 6 Flowchart of the Optimization method

performed, each optimized result will be different, but the trend of optimized results can be observed. Then, new bounds of the parameters can be obtained based on those optimized results. The final optimized results can be obtained by checking the trend of the optimized results.

Test:	Target Values	Optimized Values	Error
Focus Test 1: 1- Vickers 70.3 2- Vickers 60	E=50 GPa $\sigma$ =300 MPa n=0.1 k <sub>11</sub> =14.09 k <sub>21</sub> =3.14 k <sub>12</sub> =6.67 k <sub>22</sub> =3.10	E=50.47 GPa $\sigma$ =312.4 MPa n=0.133 k <sub>11</sub> =13.25 k <sub>21</sub> =2.38 k <sub>12</sub> =6.27 k <sub>22</sub> =2.36	E=0.95% $\sigma$ =4.16% n=33.35%
Focus Test 2: 1- Vickers 60 2- Conical 70.3	E=50 GPa $\sigma$ =300 MPa n=0.1 k <sub>11</sub> =6.67 k <sub>21</sub> =3.10 k <sub>12</sub> =34.88 k <sub>22</sub> =4.05	E=44.1 GPa $\sigma$ =281.3 MPa n=0.098 k <sub>11</sub> =7.23 k <sub>21</sub> =3.19 k <sub>12</sub> =37.82 k <sub>22</sub> =4.16	E=11.79% $\sigma$ =6.23% n=1.57%
Focus Test 3: 1- Conical 60 2- Vickers 70.3	E=50 GPa $\sigma$ =300 MPa n=0.1 k <sub>11</sub> =14.87 k <sub>21</sub> =4.22 k <sub>12</sub> =14.09 k <sub>22</sub> =3.14	E=48.44 GPa $\sigma$ =313.2 MPa n=0.115 k <sub>11</sub> =14.32 k <sub>21</sub> =3.72 k <sub>12</sub> =13.58 k <sub>22</sub> =2.77	E=3.13% $\sigma$ =4.39% n=15.3%
New Bounds	$\left\{ \begin{array}{l} 23 \text{ GPa} \leq E \leq 70 \text{ GPa} \\ 148 \text{ MPa} \leq \sigma_y \leq 445 \text{ MPa} \\ 0.06 \leq n \leq 0.17 \end{array} \right\}$		
Final Test: Based on Focus Test 1	E=50 GPa $\sigma$ =300 MPa n=0.1 k <sub>11</sub> =14.09 k <sub>21</sub> =3.14 k <sub>12</sub> =6.67 k <sub>22</sub> =3.10	E=47.3 GPa $\sigma$ =291.3 GPa n=0.105 k <sub>11</sub> =14.54 k <sub>21</sub> =3 k <sub>12</sub> =6.87 k <sub>22</sub> =2.97	E=5.36% $\sigma$ =2.9% n=5%

Table 2 Case 1 target and optimized values used in this study

In this study, a three-parameter optimization with different target values has been performed. Table 2 shows the target and optimized values used in case 1 and the other cases are presented in Appendix A.

Figure 7 shows the differences between the optimized and the experimental (target) results. There are good agreements for the loading curves for the Vickers indenter, but the unloading curves are not in good agreement. Furthermore, it is interesting to observe that the optimized portions of the loading curves for the conical indenter are slightly lower than the target curves, whereas the unloading curve is well matched. This is due to the error of the  $k_1$  coefficient and, therefore, ‘focus test 2’ can be performed by adding an upper bound to  $k_1$  factor to give better solutions.

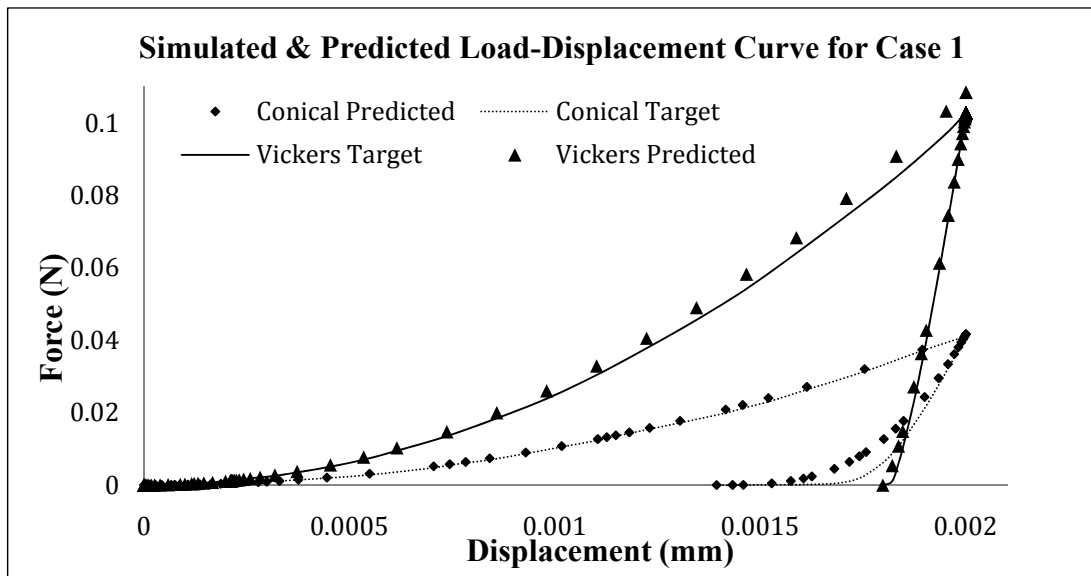


Figure 7 Comparison between the target and predicted results of focus test 1 for Case 1

### 4.3 Discussion of the results

Three material cases have been used to extract the mechanical properties from loading-unloading indentation curves. During the ‘focus test’, the accuracy of the optimized values appears to be random, but the error does not exceed 50%. In particular, the  $k$  factors are always found with a low error due to the equality constraint, shown in Eq. (19). In addition, the inequality constraint can be used if the optimized values are not reliable. In case 2 with focus test 2 in Appendix A, the first optimized values of  $k_1$  are very far away from the target values, but by using the inequality constraints, better solutions are obtained. It is always better to start with the minimum bounds of the constraint in order to achieve convergence easily, and it is noted that more accurate results can be obtained if more information of the  $k$  factors is available.

Once three focus tests have been performed, the average of the optimized values can be used as the initial guess values for the final test with new bounds. The lower and upper bounds of the parameters always start at about 100% away from the average of the updated results. Then, at every optimization loops, the bounds are reduced around the recently optimized results of the previous loop. Therefore, the final test usually converges much quicker than the earlier tests. In case 3 in Appendix A, the first final optimized results are about 20% away from the target values due to  $k$  coefficients being 10% away from their target values. By using the inequality constraints, the final optimized values reach the target values.

Although the target values are already known in this study, the optimization algorithms are also applicable to unknown target values, due to the fact that some trends can be found from the three ‘focus tests’. If those results are not reliable, more ‘focus tests’ and different types of indenters with different face angles can be used to determine more accurate optimized results. Overall, the proposed optimization method can evaluate the material properties with good accuracy.

However, the algorithms are sensitive to most of the initial guess parameters and algorithm options. In order to reduce the sensitivity of the optimization process, initial guess values and the bound parameters should not be chosen randomly. It appears that the bounds of the parameters are related to the material of specimen and the geometry of indenter. In all cases, setting about 50% boundaries of target values allows a better solution to be found. Furthermore, the characteristics of the indentation curves and the interaction of the indenter geometry with the specimen should be investigated to arrive at suitable bounds.

## 5 Conclusions

This study presents a novel optimization algorithm to extract the elastic-plastic mechanical properties from loading-unloading curves from conical and Vickers indenters with face angles of  $60^\circ$  and  $70.3^\circ$  without using dimensional functions. It is assumed that the loading and unloading curves significantly depend on the mechanical properties  $(E, \sigma_y, n)$ , and the  $k$  factors have been introduced instead of complicated dimensional functions. Based on these parameters, sets of mathematical fitting functions for the loading-unloading curves can be devised. This new algorithms is based on the Fimincon function with interior-point algorithm in MATLAB with a nonlinear least square routine with practical equality and inequality constraints.

To overcome the issue of uniqueness when using a single indenter, two different types of indenters with different face angles have been used; Vickers and conical indenters with face angles of  $60^\circ$  and  $70.3^\circ$ . The results from a single optimization loop do not give accurate solutions despite using two different indenter geometries. Therefore, an optimization algorithm based on several loops with different input tests has been introduced as ‘focus tests’. These tests can reduce the bounds of the mechanical parameters to find the optimum results. However, some limitations of this algorithm still exist due to the  $k$  factors. Therefore, a parametric study of the  $k$

factors and further work for investigating the relationships between the material properties of the specimen and the geometry of the indenter are required. This further study can help to reduce the number of unknowns and the bounds of the parameters leading to improved accuracy of the optimization results.

## References

- [1] J.J. Kang, A.A. Becker and W. Sun, “A combined dimensional analysis and optimization approach for determining elastic-plastic properties from indentation tests”, *J. Strain Analysis*, 46(8), 749-759, 2011.
- [2] J.J. Kang, A.A. Becker and Wei, Sun, Determining Elastic-plastic properties from Indentation data obtained from Finite Element Simulations and Experimental Results. *Int. J. Mech. Sci.* (Submitted)
- [3] W.C. Oliver and G.M. Pharr, “An Improved Technique for Determining Hardness and Elastic Modulus Using Load and Displacement Sensing Indentation Experiments”, *J. Mater Res*, 7(6), 1564-1583, 1992.
- [4] Matlab, “Optimization toolbox TM 4 users guide”, T.M.Inc., 2008.
- [5] M. Dao, N. Chollacoop, K.J. Van Vliet, T.A. Venkatesh and S. Suresh, “Computational modelling of the forward and reverse problems in instrumented sharp indentation”, *Acta Mater.* 49, 2899-2918, 2001.
- [6] Y.T. Cheng and C.M. Cheng, 2004, “Scaling, dimensional analysis, and indentation measurements”, *Material Science and Engineering Res*, 44, 91-149, 2004.
- [7] G.E. Dieter, “Mechanical Metallurgy”, McGraw-Hill, New York, United America, 1976.
- [8] N. Ogasawara, N. Chiba and X. Chen, “Representative strain of indentation analysis”, *J Mater Res.*, 20(8), 2225-2234, 2005.
- [9] ABAQUS, Standard 6.8-3 . “Tutorial manual version 6.8”, Pawtucket: Hibbitt, Karlsson and Sorensen, Inc., 2009.
- [10] Edlinger, M. L., Gratacos, P., Montmitonnet, P., and Felder, E. Finite element analysis of elastoplastic indentation with a deformable indenter. *Eur. J. Mech. A, Solids*, 1993, 12(5), 679–698.]
- [11] J.L. Bucaille, S. Stauss, E. Felder and J. Michler, “Determination of plastic properties of metals by instrumented indentation using different sharp indenters”, *Acta Mater.*, 51, 1663–1678, 2003.
- [12] N. Chollacoop, M. Dao and S. Suresh, “Depth-sensing instrumented indentation with dual sharp indenters”, *Acta Mater.*, 51, 3713-3729, 2003.
- [13] J. Luo and J. Lin, “A study on the determination of plastic properties of metals by instrumented indentation using two sharp indenters”, *Int. J. Solids Struct.*, 44, 5803-5817, 2007.
- [14] S. Swaddiwudhipong, K.K. Tho, Z.S. Liu and K. Zeng, “Material characterization based on dual indenters”, *Int. J. Solids Struct.*, 42, 69–83, 2005.
- [15] M.F. Ashby, “Material Selection in Mechanical Design”, 2nd ed. Elsevier, Amsterdam, 1999.

# Appendix A

## A1 Case 2

Test:	Target Values	Optimized Values	Error
Focus Test 1: 1- Vickers 70.3 2- Vickers 60	E=100 GPa $\sigma$ =900 MPa n=0.5 $k_{11}$ =11.93 $k_{21}$ =0.7 $k_{12}$ =5.77 $k_{22}$ =0.75	E=85.52 GPa $\sigma$ =866.3 MPa n=0.29 $k_{11}$ =14.69 $k_{21}$ =1.16 $k_{12}$ =7.11 $k_{22}$ =1.21	E=14.47 % $\sigma$ =3.74 % n=40.22 %
Focus Test 2: 1- Vickers 60 2- Conical 70.3	E=100 GPa $\sigma$ =900 MPa n=0.5 $k_{11}$ =5.77 $k_{21}$ =0.7 $k_{12}$ =31.41 $k_{22}$ =0.89	E=138.71 GPa $\sigma$ =569.68 MPa n=0.367 $k_{11}$ =7.26 $k_{21}$ =0.86 $k_{12}$ =39.51 $k_{22}$ =1.04	E=38.71 % $\sigma$ =36.7 % n=26.5 %
Focus Test 3: 1- Conical 60 2- Vickers 70.3	E=100 GPa $\sigma$ =900 MPa n=0.5 $k_{11}$ =11.93 $k_{21}$ =0.7 $k_{12}$ =14.47 $k_{22}$ =0.93	E=97.77 GPa $\sigma$ =983.4 MPa n=0.464 $k_{11}$ =11.71 $k_{21}$ =0.77 $k_{12}$ =14.2 $k_{22}$ =1.01	E=2.23 % $\sigma$ =9.26 % n=7.16 %
New Bounds	$\left\{ \begin{array}{l} 77 \text{ GPa} \leq E \leq 124 \text{ GPa} \\ 689 \text{ MPa} \leq \sigma_y \leq 954 \text{ MPa} \\ 0.32 \leq n \leq 0.5 \end{array} \right\}$		
Final Test: Based on Focus Test 1	E=100 GPa $\sigma$ =900 MPa n=0.5 $k_{11}$ =11.93 $k_{21}$ =0.7 $k_{12}$ =5.77 $k_{22}$ =0.75	E=100.46 GPa $\sigma$ =861.64 GPa n=0.503 $k_{11}$ =12.94 $k_{21}$ =0.7 $k_{12}$ =5.89 $k_{22}$ =0.73	E=0.4 6% $\sigma$ =5.26 % n=0.7 %

Table A1 Case 2 target and optimized values used in this study



## A2 Case 3

Test:	Target Values	Optimized Values	Error
Focus Test 1: 1- Vickers 70.3 2- Vickers 60	E=210 GPa $\sigma$ =900 MPa n=0.3 k <sub>11</sub> =13.99 k <sub>21</sub> =1.01 k <sub>12</sub> =6.56 k <sub>22</sub> =1.02	E=230.72 GPa $\sigma$ =707.38 MPa n=0.182 k <sub>11</sub> =18.25 k <sub>21</sub> =1.54 k <sub>12</sub> =8.55 k <sub>22</sub> =1.54	E=9.87 % $\sigma$ =21.4 % n=39.2 %
Focus Test 2: 1- Vickers 60 2- Conical 70.3	E=210 GPa $\sigma$ =900 MPa n=0.3 k <sub>11</sub> =6.56 k <sub>21</sub> =1.02 k <sub>12</sub> =33.82 k <sub>22</sub> =1.35	E=231.38 GPa $\sigma$ =755.42 MPa n=0.292 k <sub>11</sub> =7.133 k <sub>21</sub> =1 k <sub>12</sub> =36.773 k <sub>22</sub> =1.33	E=10.18 % $\sigma$ =16.06 % n=2.72 %
Focus Test 3: 1- Conical 60 2- Vickers 70.3	E=210 GPa $\sigma$ =900 MPa n=0.3 k <sub>11</sub> =15.44 k <sub>21</sub> =1.39 k <sub>12</sub> =13.99 k <sub>22</sub> =1.01	E=212.6 GPa $\sigma$ =865.3 MPa n=0.37 k <sub>11</sub> =14.56 k <sub>21</sub> =1.13 k <sub>12</sub> =12.72 k <sub>22</sub> =0.83	E=1.23 % $\sigma$ =3.85 % n=24.65 %
New Bounds	$\left\{ \begin{array}{l} 112 \text{ GPa} \leq E \leq 250 \text{ GPa} \\ 387 \text{ MPa} \leq \sigma_y \leq 1162 \text{ MPa} \\ 0.14 \leq n \leq 0.42 \end{array} \right\}$		
Final Test: Based on Focus Test 1	E=210 GPa $\sigma$ =900 MPa n=0.3 k <sub>11</sub> =13.99 k <sub>21</sub> =1.01 k <sub>12</sub> =6.56 k <sub>22</sub> =1.02	E=215.37 GPa $\sigma$ =825.3 GPa n=0.302 k <sub>11</sub> =14.59 k <sub>21</sub> =0.991 k <sub>12</sub> =6.84 k <sub>22</sub> =0.992	E=2.55 % $\sigma$ =8.29 % n=0.93 %

Table A2 Case 3 target and optimized values used in this study